

**Haptic Manipulation of Microspheres using Optical
Tweezers**

Under the Guidance of Artificial Potential Fields

by

Ibrahim Bukusoglu

**A Thesis Submitted to the
Graduate School of Engineering
in Partial Fulfillment of the Requirements for
the Degree of**

**Master of Science
in
Mechanical Engineering**

Koc University

October 2006

Koc University
Graduate School of Sciences and Engineering

This is to certify that I have examined this copy of a master's thesis by

Ibrahim Bukusoglu

and have found that it is complete and satisfactory in all respects,
and that any and all revisions required by the final
examining committee have been made.

Committee Members:

Asst. Prof. Dr. Cagatay Basdogan (Advisor)

Asst. Prof. Dr. Alper Kiraz

Asst. Prof. Dr. Erdem Alaca

Date:

ABSTRACT

Using optical tweezers (OT) and a haptic device, we have manipulated microspheres having diameters of 3-4 μm floating in a fluid solution in order to form different patterns of coupled optical microresonators. For this purpose, biotin-coated microspheres trapped by a laser beam are steered and bound to an immobilized streptavidin-coated anchor sphere using a piezo scanner controlled by a haptic device. The positions of all spheres in the scene are detected using a CCD camera and a collision-free path for each trapped sphere is generated using an artificial potential field. The forces acting on the trapped particle due to the viscosity of the fluid and the artificial potential field are scaled and displayed to the user through the haptic device for better guidance and control during steering. A virtual fixture is used to exert forces on the user to guide him/her while binding the trapped sphere to the anchor one such that the desired angle of approach and binding strength are achieved. The proposed system is used to assemble microspheres with controlled manipulation and accurate alignment. Our experimental studies in virtual and real environments with 8 human subjects show that haptic feedback significantly improves the user performance by reducing the task completion time, the number of undesired collisions during steering, and the positional errors during binding. Due to high positioning accuracy, the proposed haptic manipulation techniques can find use in constructing coupled microsphere resonators or

coupled resonator optical waveguides. To our knowledge, this is the first study in the literature demonstrating the benefits of haptic guidance in optical trapping and manipulation.

ACKNOWLEDGEMENTS

I would like to begin by thanking my advisor Asst. Prof. Dr. Cagatay Basdogan for his support and guidance throughout my thesis study. I thank him for his suggestions and discussions about my research activities.

I am grateful to Assist. Prof. Dr. Alper Kiraz for his help and support throughout my thesis and making the laboratory available when I needed.

I also would like to thank Adnan Kurt for his helps about the instrumentation during my study

I would like to thank Asst. Prof. Dr. Halil Kavakli and Şule Özdaş for their helps during the coating processes in the Biology Laboratory.

I would like to thank all the faculty and students in the department of Mechanical Engineering in Koç University, for their passion to help and share knowledge. Special thanks go to İhsan, Murat, Ozan, Tarkan, Aydın, Buğra, Mustafa and Durul for their help in my thesis work.

Last, I am very grateful to my family, and my special friends for their love and support.

TABLE OF CONTENTS

List of Tables	viii
List of Figures	ix
Nomenclature	x
Chapter 1: Introduction	1
Chapter 2: Experimental Set-up	7
2.1 Set-up	7
2.2 Calibration of the Set-up	12
2.3 Optical Manipulation with Haptic Feedback.	16
2.3.1 Path Planning Forces	16
2.3.2 Drag Forces	19
2.3.3 Virtual Fixtures	19
2.3.4 Constructing Microsphere Assemblies.	21
Chapter 3: Experimental Study	23
3.1 Experiment I.	24
3.1.1 Goal	24
3.1.2 Design	24

3.1.3	Procedure	26
3.1.4	Results.	27
3.2	Experiment II.	31
3.2.1	Goal	31
3.2.2	Design	31
3.2.3	Procedure	32
3.2.4	Sample Preparation	34
3.2.5	Results.	35
Chapter 4: Discussions and Conclusion		39
Bibliography		43
Vita		46

LIST OF TABLES

Table 3.1: The Matrix design for Experiment I	26
Table 3.2: Comparison of success rates for Experiment I	36

LIST OF FIGURES

Figure 1.1: a) Whispering Gallery Mode (WGM), b) Emission Spectrum	5
Figure 2.1: Experimental Set-up	8
Figure 2.2: Flowchart for the Software	10
Figure 2.3: The output after each step	11
Figure 2.4: Calibration results	13
Figure 2.5: Optical Trapping	15
Figure 2.6: a) Potential Field, b) Attractive and Repulsive Forces	18
Figure 2.7: Virtual Fixtures	20
Figure 2.8: a) Assembly of microspheres using biotin-streptavidin binding. b) Constructed patterns	22
Figure 3.1: Design of Experiment I	25
Figure 3.2: Results of Experiment I	29
Figure 3.3: Effect of Haptic Feedback on Learning	30
Figure 3.4: Manipulation Screen for Experiment II	33
Figure 3.5: The quantities measured in Experiment II	37
Figure 3.6: Results of Experiment II	38

NOMENCLATURE

λ	wavelength (nm)
NA	numerical aperture
F_{DRAG}	drag force (N)
η	viscosity
v	velocity (m/sec)
r	radius (m)
F_{TRAP}	trap force (N)
k	trap stiffness (N/m)
Δx	difference between the centers
$U(q)$	artificial potential field
$U_{goal}(q)$	artificial potential field related to the goal point
$U_{obstacle}(q)$	artificial potential field related to obstacles
F_{att}	attractive force field
F_{rep}	repulsive force field
$g(q)$	shortest distance to the obstacle
q_0	radius of influence
q_z	location of the obstacle
β, α	gain

Chapter 1

INTRODUCTION

Optical Tweezers (OT) are a single beam optical trap used to immobilize or transport objects in three dimensions. The first optical trap was built by Ashkin in 1970. He showed that small dielectric particles can be accelerated by the radiation pressure of a laser beam and trapped by two counter propagating beams. In 1986, Ashkin, Dziedzic, Bjorholm and Chu again succeeded in trapping particles using a single, highly focused laser beam known as OT. The basics of optical trapping using OT are quite straightforward for both objects smaller and larger than the wavelength of light. A laser beam is focused by a high numerical aperture microscope objective to a spot in the plane of specimen. This spot creates an optical trap which is able to hold a small particle at its focus. The electric dipole moment in response to the light's electric field creates a force towards the focus of the light beam on the objects. For small objects, the trapping force is given by the gradient of the electric field, while for large objects it can be visualized as the reaction to the net momentum change of photons passing through the particle. This force, always acting towards the focus, moves the particle or immobilizes it when the beam is moved or the manipulation environment is moved while the trap is stationary. The majority of OT make use of conventional TEM₀₀ Gaussian beams to trap particles. Laguerre Gaussian beams are also used in the OT to give them the ability to trap and manipulate objects that are optically reflective or absorptive. Laguerre Gaussian beams have a well defined orbital angular momentum that can rotate trapped objects. Also zero or higher order Bessel beams are used in the OT to rotate

multiple particles apart from each other and around obstacles [3]. A single-trap standard OT have one or at most two laser beams. On the other hand, multiple trap OT (i.e. Holographic OT) are made possible by sharing a single beam in temporal or spatial space using acousto-optic deflectors or galvanometer driven mirrors [4].

OT are suitable for manipulating objects with length scales ranging from tens of nanometers to micrometers and exerting forces on the objects ranging from femtonewtons to nanomewtons [5]. As a result of these features, along with its non invasive nature (because no physical contact is present), OT have found applications in many fields. They are highly attractive for investigating biological systems since the scale of the applied forces are highly small [6] For example, OT have been used to probe the viscoelastic properties of single biopolymers (such as DNA), cell membranes, aggregated protein fibres (such as actin), gels of such fibres in the cytoskeleton, and composite structures (such as chromatin and chromosomes). They have also been used to characterize the forces exerted by molecular motors such as myosin, kinesin, processive enzymes and ribosomes. OT can also be used to construct patterns by assembling micro particles. These patterns can be used later as building blocks for constructing micro devices as proposed, but not implemented, in the work by Castelino et al [4].

Manipulating micro scale particles using OT and visual feedback is highly challenging. When an external force is applied to a particle trapped by a laser beam, the particle is displaced from the focus of the beam in a manner similar to an object that is attached to a mechanical spring and exposed to an external force. In addition, a drag force acting on the particle (note that particles are floating in a fluid solution) during steering makes the manipulation more difficult. If the manipulation velocity is high, the particle may escape from the trap. Moreover, if two particles are intended to be bound to each other as in some biological applications, one must not only avoid undesired collisions with other particles during steering, but also align particles precisely during binding. For example, Bryant et al.

binds two DNA coated microspheres to each other using a pipette and visual feedback to measure the mechanical properties of DNA. He measures the forces acting on the trapped sphere in X and Y directions using a photo-detector and displays them as graphical bars on the computer monitor to check if the molecular binding has occurred [7]. Force and position control is also necessary if a micro or nanoscale object is to be attached to or inserted into a biological entity. For example, Pauzauskie et al. use OT to insert a fluorescent nanowire into a cell for tracking its movements in the body. They bring the wire close to a human cervical cancer cell and then push it carefully for several seconds to penetrate inside the cell without damaging it [8]. As it is obvious from these examples, in many applications of OT, collision-free steering, accurate positioning, and force control are necessary for the successful execution of the task.

To this end, haptic feedback appears to be a natural choice [9]. During the steering and assembly operations, we display to the user the drag force acting on the trapped sphere and guidance forces due to an artificial potential field and a virtual fixture through a haptic device to help him/her manipulate the sphere more effectively and efficiently. Under the guidance of these forces, the trapped microsphere is steered along a collision free path and bound to an anchor sphere along a pre-calculated line specifying the angle of contact. The virtual fixture pulls the trapped sphere towards this line when the sphere is sufficiently close to the anchor sphere. Virtual fixtures have been shown to improve user performance and learning in telemanipulation tasks and training tasks simulated in virtual environments [10, 11, 12]. They have also been shown to be effective in robot programming and demonstration [13].

We demonstrate a novel application of haptic guidance in optical manipulation of microparticles under the influence of artificial force fields for accurate assembly of microspheres. The achieved high positioning accuracy can find use especially in assembling coupled microsphere resonators or coupled resonator optical waveguides.

In a single sphere optical resonator, light confined in the spherical volume with an index of refraction greater than that of the surrounding medium exhibits resonances called as Whispering Galley Modes (WGMs) [14]. WGMs can be observed by analyzing the emission spectrum of the fluorescent molecules doped inside a microsphere. As shown in Figure 1 high intensity peaks observed in the collected emission indicate the WGMs. An important parameter of an optical resonator is its quality factor Q which is defined as $\omega/\Delta\omega$, where ω is the angular frequency at a particular wavelength. An ideal resonator would confine light indefinitely (without loss) leading to an infinite Q . However, infinite Q cannot be reached because of the absorption, reflection, and scattering losses [15].

Microsphere resonators are systems where high Q factors can be achieved together with very small mode volumes. These yield them very attractive for applications in atom optics, quantum electrodynamics, optical communication, and biology. Some applications of the resonators in these fields include microlasers, narrow filters, optical switching, displacement measurements, raman sources, studies of nonlinear optical effects and ultrafine sensing. The research in this area has recently focused on investigating different patterns of micro resonators assembled from multiple microspheres (i.e. coupled microsphere resonators, coupled resonator optical waveguides). Möller, Woggon, and Artemyev showed the changes in the emission spectrum of exactly size matched microspheres doped with CdSe quantum dots arranged in different orientations [16]. They also demonstrated waveguiding of WGMs using coupled microspheres. In these demonstrations, microspheres are assembled by a self-assembly process which relies on mixing the spheres in a solution of methanol and leaving the solution to dry to form random patterns. The self-assembly process has two major drawbacks: First, the nature of the process prevents accurate alignment of the patterns. Accurate alignment is very important as it determines the coupled optical modes in coupled microsphere resonators. Furthermore, in a coupled resonator optical waveguide structure the waveguiding is determined by the alignment of the microspheres. Second, the variety of

patterns that can be formed is limited, and complex patterns cannot be constructed by self-assembly. This limits the number of resonators that can be constructed for different applications. As an alternative to self-assembly, we propose to use haptic feedback with OT to manipulate spheres in a controlled manner. In this technique, we convey to the user the drag forces acting on the sphere as well as the forces due to the artificial potential field and virtual fixtures during the steering and assembly of microspheres. As we demonstrate, this helps the user manipulate the spheres more effectively in assembling different patterns.

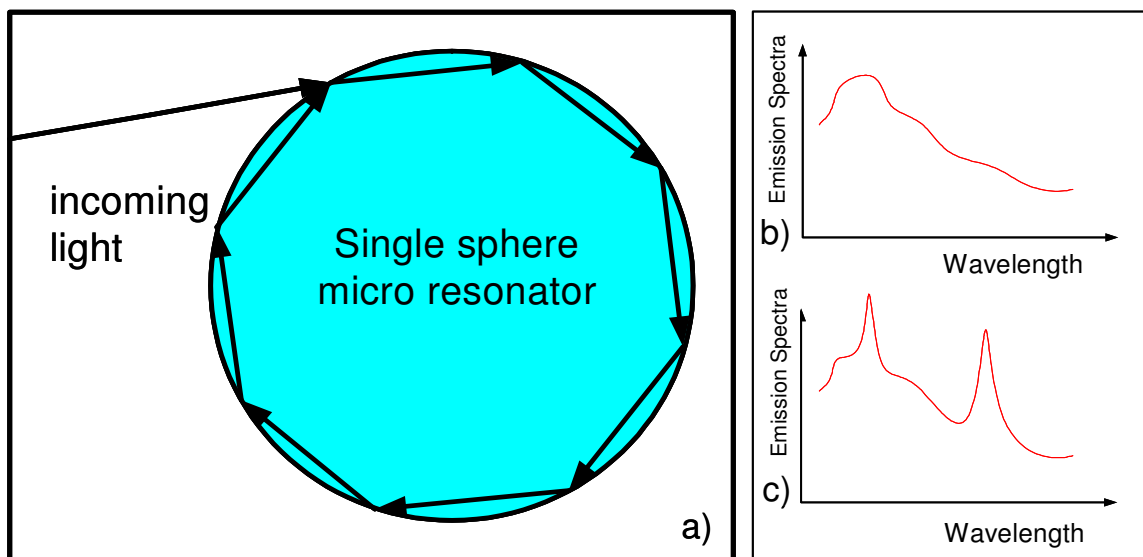


Figure 1.1 : a) Whispering Gallery Modes (WGMs): At these resonant wavelengths, the light undergoes total internal reflection inside the sphere and folds back on itself in phase. The emission spectra of an atom before (b) and after (c) entering an optical cavity (representative). The resonant modes at two different wavelengths are apparent in (c).

The remainder of the thesis is organized as follows: Chapter 2 describes the experimental setup for manipulating microspheres using OT and a haptic device. We discuss the calibration of the setup which is necessary to determine the trapping stiffness and the maximum velocity that can be attained during the manipulation of spheres and the haptic assistance modes, including an artificial potential field used for steering and a virtual fixture used for binding. Chapter 3 presents the design, procedure, and results of two experiments conducted in virtual and real environments to investigate the role of haptic guidance in steering and binding processes. Finally, the discussion of the results and the conclusions are given in Chapter 4.

Chapter 2

EXPERIMENTAL SETUP

2.1 Setup

The set-up for the proposed manipulation system is shown in Figure 2.1. The system consists of two major parts: OT and a haptic interface. For the OT, the beam of a continuous wave green laser (Crysta Laser CRL-GCL-025-L, $\lambda = 532$ nm) with an output power of 25 mW is sent through a 6x magnifying telescope into an inverted microscope (Nikon TE 2000-U). After being reflected off a dichroic mirror (Chroma Filters Q570LP), the laser beam is focused on the sample by a high numerical aperture (NA = 1.4, 60x) microscope objective. This beam is used to trap microspheres for manipulation. The images of the spheres are captured by a CCD camera. By using an intermediate magnification module, a total magnification of 90x is achieved. A red pass filter (Chroma filters HQ610/75) is used to filter out stray laser light. In our system, the location of the laser beam is fixed and the movements of a particle trapped by the beam is controlled by a three-dimensional piezoelectric scanner (Piezosystem Jena Tritor 102-SG) working in the closed loop control (scanning resolution is 2 nm). The movements of the scanner are commanded by the user via a haptic device (Omni haptic device from Sensable Technologies Inc.) The displacements of the haptic stylus are scaled and suitable voltage values are sent to the scanner to control its movements on the sample plane. The forces acting on the trapped particle during the manipulations are conveyed to the user through the same haptic device.

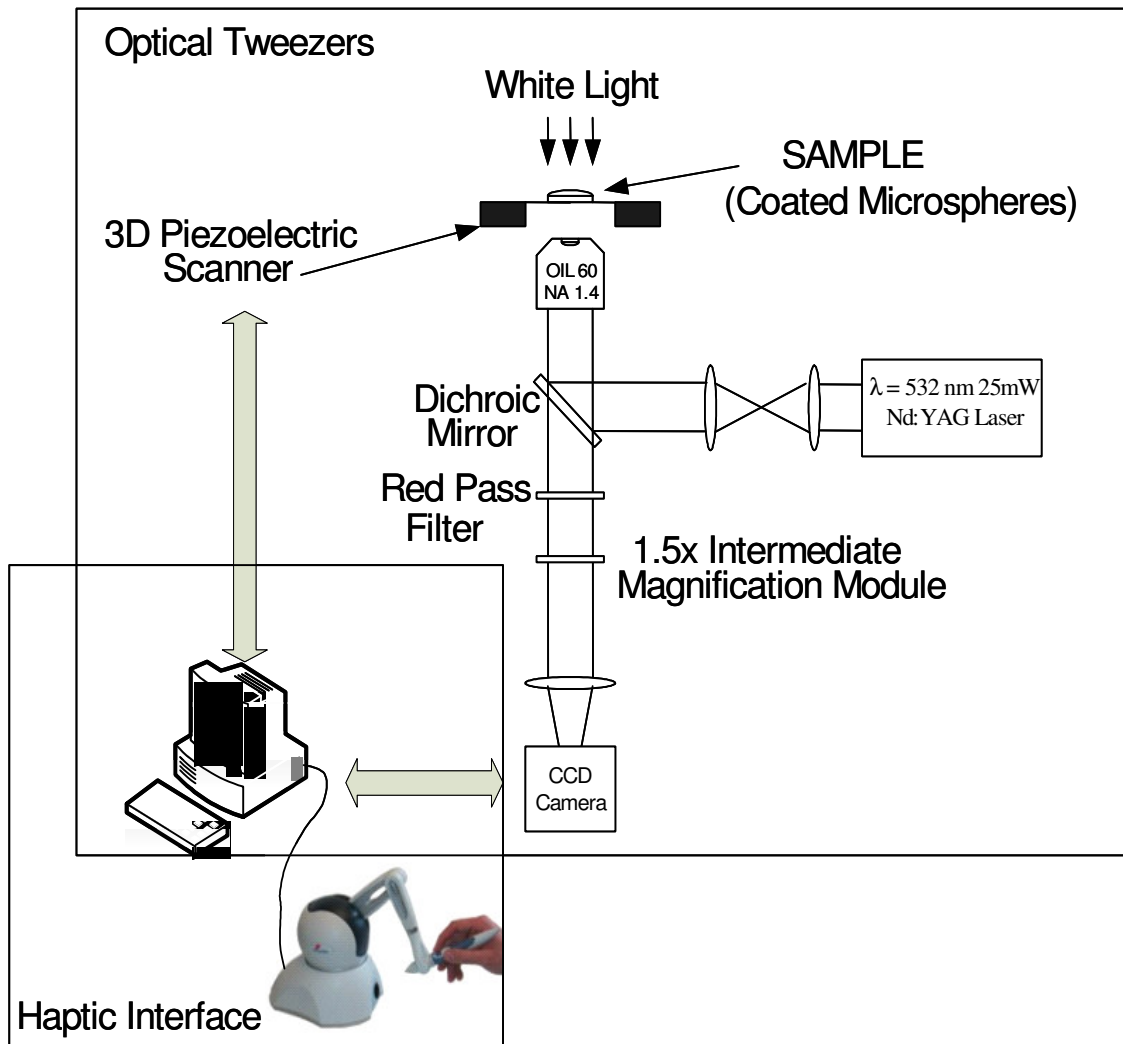


Figure 2.1: The experimental set-up for manipulating microspheres include OT and a haptic device. The haptic device controls the movements of the 3D piezo scanner with respect to the laser trap and display guidance forces to the user during the real-time manipulations.

The synchronized working of the different components of the manipulation system is accomplished by a computer program written in C++ language. The flowchart of the program is given in Figure 2.2. First, a snapshot of the manipulation environment is captured via the CCD camera. Then a threshold is applied to the captured image and the center position and radius of each microsphere in the image are calculated using a contour finding algorithm. Using this information, a virtual model is constructed to provide the user with the bird's eye view of the manipulation environment during the execution of the task. Since the CCD camera is fixed and not moving with the scanner, the user may easily lose the "big picture" during the manipulation of a sphere without a bird's eye view. The user then enters the required inputs according to the manipulation task he/she wants to perform. For example, a target location is entered for a steering task. If the task also involves an assembly, then the location of anchor spheres and the binding angles are specified. Based on the input parameters, the computer program automatically generates an artificial potential field and virtual fixtures to provide haptic guidance to the user for better execution of the task. In each step of the manipulation, the haptic loop acquires the position and velocity of the stylus and calculates the appropriate forces to be exerted on the user. Figure 2.3 shows the output after each step.

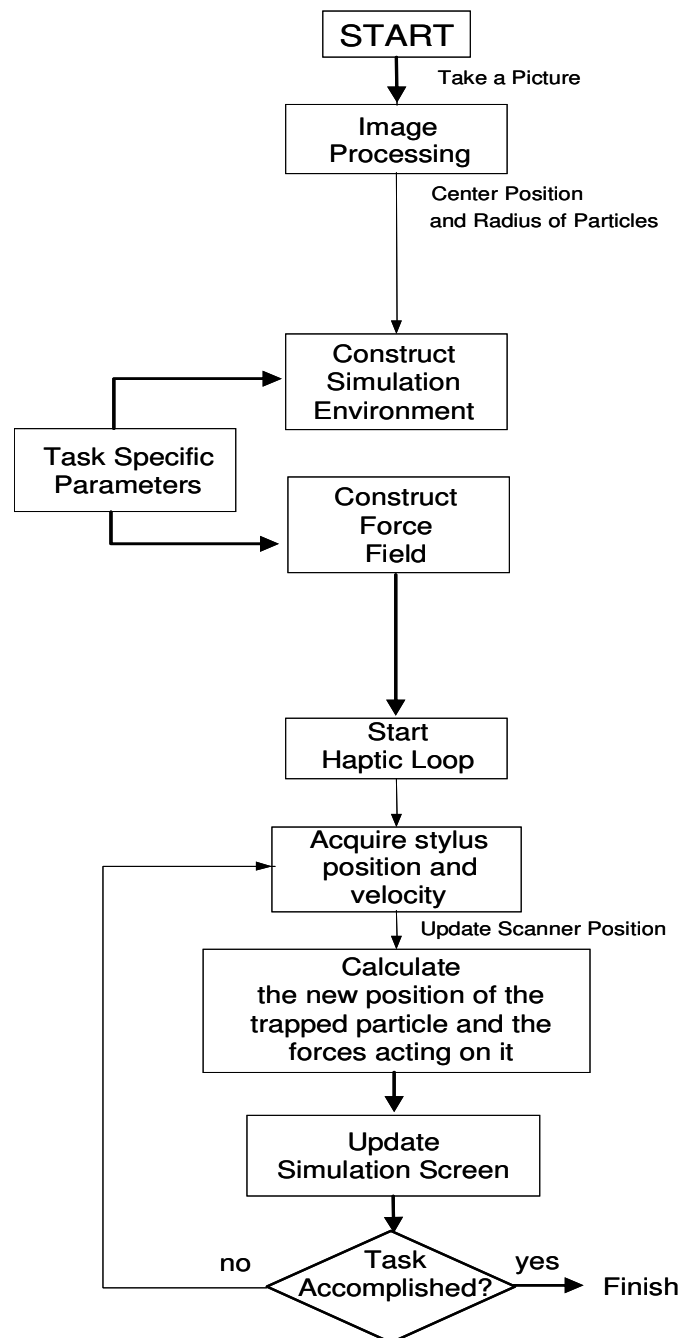


Figure 2.2 : The flowchart for the Software

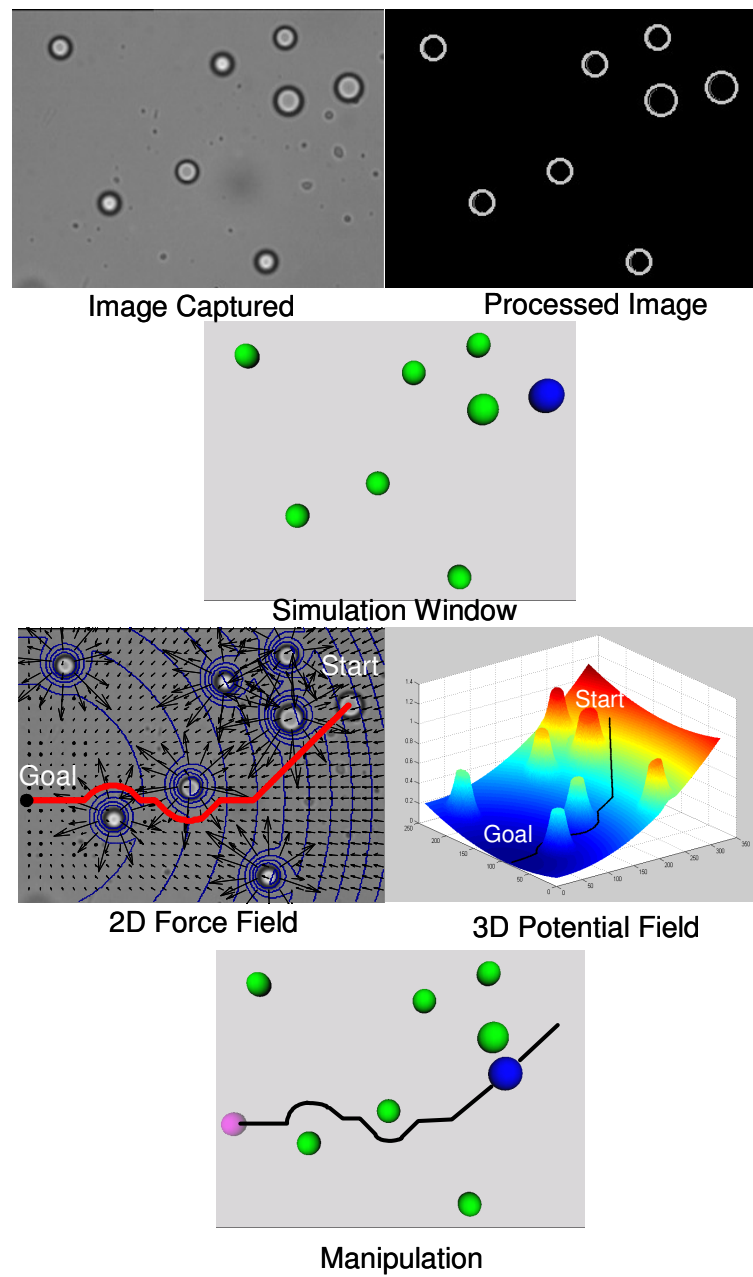


Figure 2.3 : The output after each step.

2.2 Calibration of the Set-up

The system must be calibrated in order to find the limits of the manipulation. Since the manipulation process is carried out in an aqueous solution, drag forces acting on the trapped particle may exceed the forces applied by the laser beam if the particle is manipulated with a high velocity. As a result, the particle may escape from the trap. In order to avoid this, first the maximum trapping force and spring constant of the trap must be determined in advance by calibrating the system and then the speed of the particle must be controlled accordingly. There are various techniques available for calibrating OT. One of them is the power spectrum method that takes advantage of the Brownian motion of the trapped particles to calculate the stiffness of the optical trap. Another one is the equipartition method which utilizes the thermal fluctuations of the particles to calculate the stiffness of the trap. In order to use these methods, an accurate and high speed sensing of the particle position is necessary which is typically achieved by using a quadrant photo detector. An alternative, but typically less accurate, approach is to use camera images to determine the position of the trapped sphere. The calibration approach that is most appropriate to use with the camera images is the escape force method [17]. In this method, a trapped particle is moved away from the cover slip such that the distance between the particle and the cover slip is much larger than the radius of the particle. Then, the scanner is commanded to move in different velocities until the particle escapes from the trap. The displacement of the particle from the center of the beam is measured for the different velocities (Figure 2.4). The drag force applied on the particle is calculated using the Stokes law, $F_{\text{DRAG}} = 6\pi\eta rv$, where η is the viscosity of the fluid, v is the velocity of the scanner and r is the radius of the particle. The particle escapes from the trap at a velocity of 100 μ /sec. A correction factor is typically applied to the escape velocity according to the Faxen's law for the spherical objects manipulated close to a cover slip [18]. The correction

factor for our application is calculated as 2.36. After the correction, the maximum velocity for controlled manipulation of a particle in our optical trap is calculated as $42 \mu\text{/sec}$ ($100/2.36$).

In addition to drag forces acting on the particle, there are trapping forces exerted by the laser beam. A laser beam exerts gradient and scattering forces on the object. Small objects with sizes comparable to laser wavelength develop an electric dipole moment in response to the light's electric field. This leads to a gradient force which attracts the particle to the beam focus with a magnitude proportional to the intensity gradient of the laser beam. Larger objects such as the microspheres used in our experiments act as lenses, causing to a

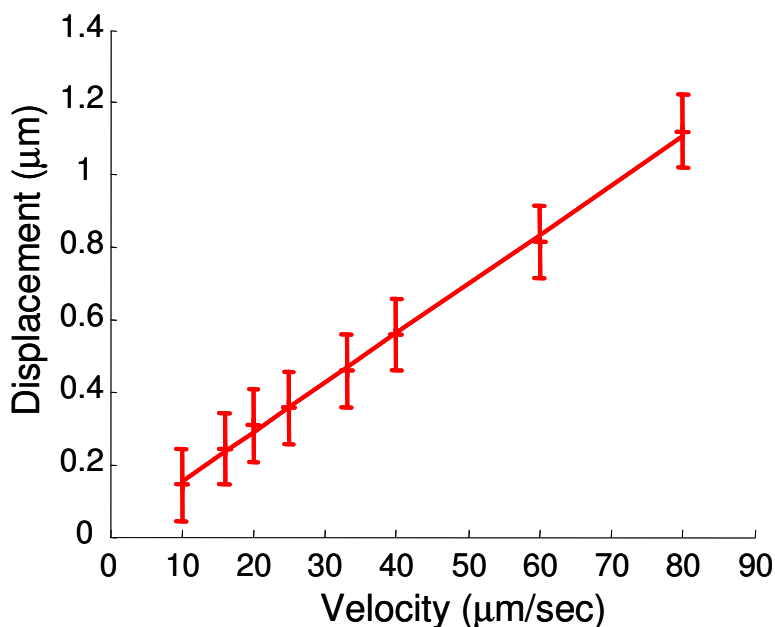


Figure 2.4 : The OT must be calibrated to calculate the spring constant of the laser trap and the maximum manipulation speed. For calibration, the piezo scanner is commanded to move at increasing speeds until the particle escapes from the trap and the difference between the centers of the laser beam and the trapped particle are recorded.

change in the momentum of the incident photons. This results in an effective force which draws the particle towards the higher flux of photons near the focus [6]. For the inverted geometry depicted in Figure 2.5a, the particle reaches equilibrium along the axis of the laser beam (z-axis) by the gradient, scattering, and the gravitational forces. As long as the particle is at the center, the intensity of the light around the particle is symmetric and hence the gradient forces cancel each other resulting in a forward force (scattering force) which is balanced by the weight of the particle (Figure 2.5b). However, when the center of the trapped particle and the laser beam is not coincident, the gradient force pulls the particle to the center of the beam (Figure 2.5c). This force can be modeled as a spring and formulated as $F_{\text{TRAP}} = k \Delta x$, where k is the stiffness of the trap and Δx is the difference between the centers. During the calibration experiments, the drag force acting on the trapped particle is balanced by the gradient forces exerted by the laser beam. The stiffness of the trap is calculated by dividing the drag force with the distance between the center of the beam and the center of the particle (Δx). As a result, the trap stiffness is calculated as 4.4 pN/ μm .

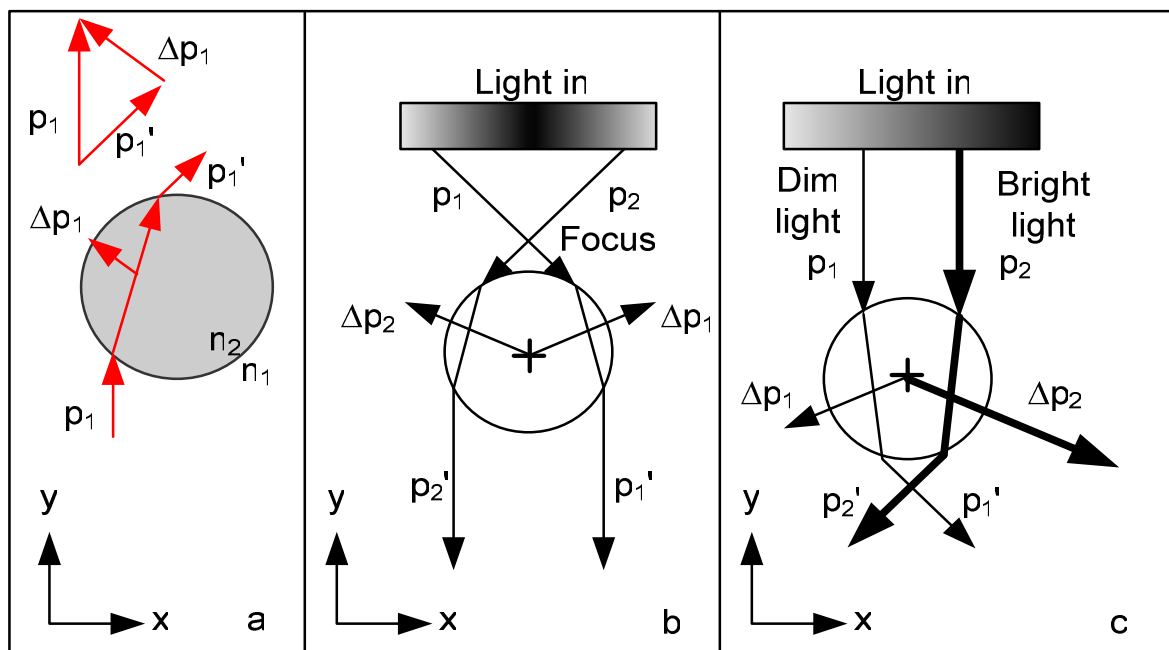


Figure 2.5 : For the ray optics regime (the diameter of the trapped particle is much larger than the wavelength of the incident light), a single ray can be tracked through the particle. If the ratio of the refractive index of the particle to the refractive index of the medium surrounding it is sufficiently large diffraction effects can be neglected. In order to satisfy this condition particles to be manipulated are put into an aqueous solution such as water. The incident laser beam can be decomposed into individual rays according to their intensity (at the center of the beam the most intense light is present. A logarithmic decay occurs as the distance from the center is increased). After a ray travels through the particle the momentum of the photons are changed and the force due to this change applies forces on the particle which has components in both the forward (scattering force) and side (gradient force) directions (see the X and Y components of ΔP_1 in Figure a). As long as the particle is at the center (Figure b), the intensity of the light around the particle is symmetric and because of that the gradient forces (see X components of ΔP_1 and ΔP_2) cancel each other resulting in a forward force (the summation of Y components of ΔP_1 and ΔP_2) which is balanced by the weight of the particle. However, when the particle is eccentric according to the beam, the net force on the particle creates a gradient force which always pulls the particle to the center of the beam (Figure c). Hence, as the laser beam is moved, the particle, under the effect of this gradient force, moves with the laser. Or, the laser beam trapping a particle is fixed, but a piezo scanner moves the other particles with respect to the trapped particle as in our case.

2.3 Optical Manipulation with Haptic Feedback

The haptic device in our set-up controls the movements of the scanner to manipulate the particles and also provides force feedback to the user during the manipulations. In order to assemble microspheres to construct micro resonators, two different types of manipulations are necessary: a) the spheres must be transported to the target locations (steering) and then b) must be attached to each other by chemical means (binding). To help the user to steer the particles while avoiding the collisions with the others, we use a potential field approach. During the binding, virtual fixtures are used to enable the user to position the particles precisely first and then apply controlled forces to the particles to make the binding possible. Hence, the forces conveyed to the user during the manipulations can be classified in three groups: the forces due to a) the artificial potential field (i.e. path planning forces), b) virtual fixtures, and c) viscous drag of the fluid.

2.3.1 Path Planning Forces

For individual steering of particles, we have implemented a path planning algorithm based on a potential field approach. This is a well-known approach in robotics used for motion and path planning [19]. Potential field approach involves the modeling of the position to be reached as an attractive pole and obstacles as repulsive surfaces. In this approach an artificial potential field $U(q)$ is constructed from the components associated with the goal ($U_{\text{goal}}(q)$) and any obstacles ($U_{\text{obstacles}}(q)$). The net potential felt by the particle is:

$$U(q) = U_{\text{goal}}(q) + \sum U_{\text{obstacles}}(q) \quad (1)$$

where, q is the location of a point in the potential field

The force acting on the particle in the case of a 2D problem is

$$F = -\nabla U(q) = -\begin{pmatrix} \frac{\partial U}{\partial x} \\ \frac{\partial U}{\partial y} \end{pmatrix} \quad (2)$$

Typically U_{goal} is defined as a parabolic attractor

$$U_{\text{goal}}(q) = \frac{1}{2} \alpha \text{dist}(q, \text{goal})^2 \quad (3)$$

$$F_{\text{att}}(q) = -\nabla U_{\text{goal}}(q) = -\alpha (q - q_{\text{goal}}) \quad (4)$$

where, α is the gain

The repulsive force of an obstacle is typically modeled as a potential barrier that arises to infinity as the particle approaches the obstacle. It is also desired that the repulsive potential does not affect the motion of the robot when it is sufficiently away from the obstacles. Then the repulsive field is defined as below:

$$U_{\text{rep}}(q) = \begin{cases} \frac{1}{2} \beta \left(\frac{1}{g(q)} - \frac{1}{q_0} \right) & \text{if } g(q) \leq q_0 \\ 0 & \text{if } g(q) > q_0 \end{cases} \quad (5)$$

where

$g(q)$: $\min \|q - q_z\|$ (shortest distance to the obstacle)
 q_z : location of the obstacle
 q_0 : radius of influence
 β : gain

$$F_{\text{rep}}(q) = + \begin{cases} \beta \left(\frac{1}{g(q)} - \frac{1}{q_0} \right) \frac{1}{g^2(q)} \nabla g(q) & \text{if } g(q) \leq q_0 \\ 0 & \text{if } g(q) > q_0 \end{cases} \quad (6)$$

The repulsive force can be modeled as a nonlinear spring between the manipulated particle and each obstacle in the field (i.e. the other particles) which increases quadratically as the distance between the particle and the obstacle is reduced linearly (Figure 2.6). As a result of the repulsive forces, a possible collision with the other particles along the steering path is avoided. These collisions may result in the escape of the particle from the trap or an undesired binding of the particle to another particle. The attractive forces, on the other hand, give an intuition to the user about where he/she should go in order to reach the target location for binding as quick as possible. These two forces together create a tunneling effect and guide the user to a collision-free path.

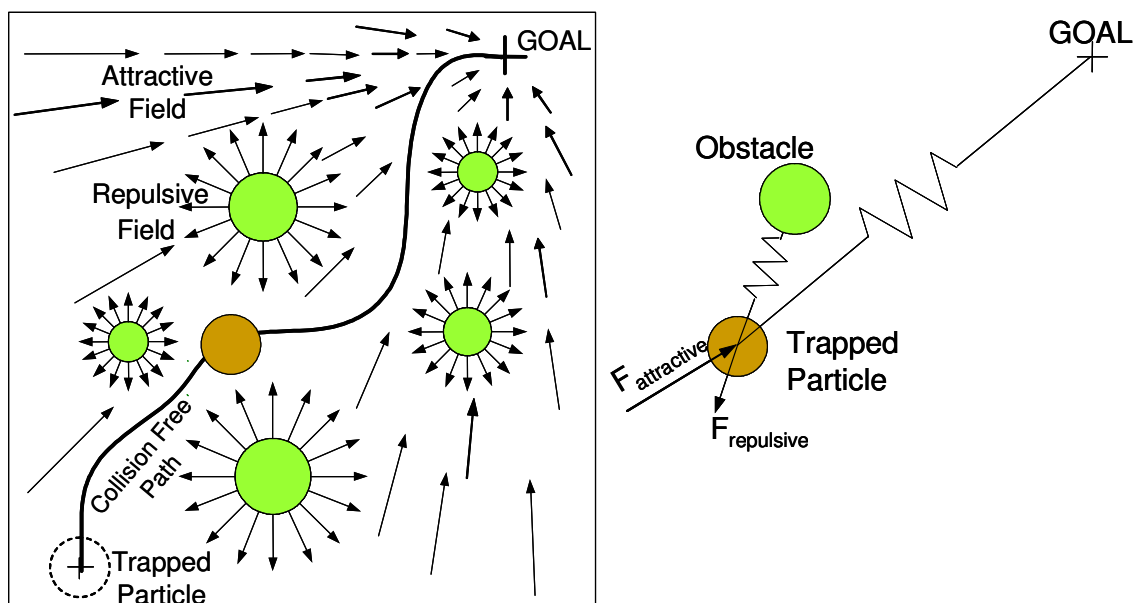


Figure 2.6 : During the steering of a trapped particle, guidance forces due to an artificial potential field are displayed to the user through the haptic device (a). The trapped particle is pulled to the goal point via attractive forces in the field while the repulsive forces around the particles along the steering path prevent the collisions (b).

2.3.2 Drag Forces

As discussed earlier, a drag force acts on the particle while it is being steered. In our system we scale these forces and give it to the user via the haptic device as he/she moves the stylus. This force gives an intuition to the user about the forces acting on the particle and limits the speed of the stylus which in turn is the speed of the particle. So the escape of the particle from the trap is eliminated and a more efficient manipulation is achieved.

2.3.3 Virtual Fixtures

The term virtual fixture refers to a software implemented guidance that help a user perform a task by limiting his/her movements into restricted regions and/or influencing its movement along a desired path [10]. The virtual fixtures can be thought of as a ruler or a stencil [20]. By the help of a ruler or stencil, a person can draw lines and shapes faster and more precisely than the ones drawn by free hand. A haptic device can be programmed to apply forces to the user to perform the same task with the help of virtual fixtures. Since the type of constraints that could be programmed to generate virtual fixtures is limited by the software only, they are more powerful than stencils.

Virtual fixtures offer an excellent balance between automated operation and direct human control. They help the operator carry out a structured task faster and more precisely or they can act as safety elements preventing the manipulators from entering dangerous or undesired regions. For example, studies on telemanipulation systems show that user performance on a given task can increase as much as 70% with the introduction of virtual fixtures [10]. The applications of virtual fixtures are in robotic assisted surgery, robot programming by demonstration, training, and telemanipulation [20].

In our system, we use a virtual fixture to provide haptic guidance to the user such that he/she stays on the correct approaching direction for the successful binding. When the distance between the manipulated trapped sphere and the one fixed on the cover slip (the

anchor sphere) is less than a threshold value, the haptic device applies forces on the user to pull him/her on a straight line which has a direction along the desired binding angle passing through the center of the anchor sphere. The user is free to move along the line, but when he/she moves out of the line, an attractive spring force proportional to the perpendicular distance between the line and the position of the microsphere is applied to him/her by the haptic device (Figure 2.7). This virtual fixture helps the user to accomplish the binding task more easily and accurately. Moreover, a repulsive field is defined for the anchor sphere to prevent the user from applying excessive forces during binding which results in escape of the binding particle from the trap.

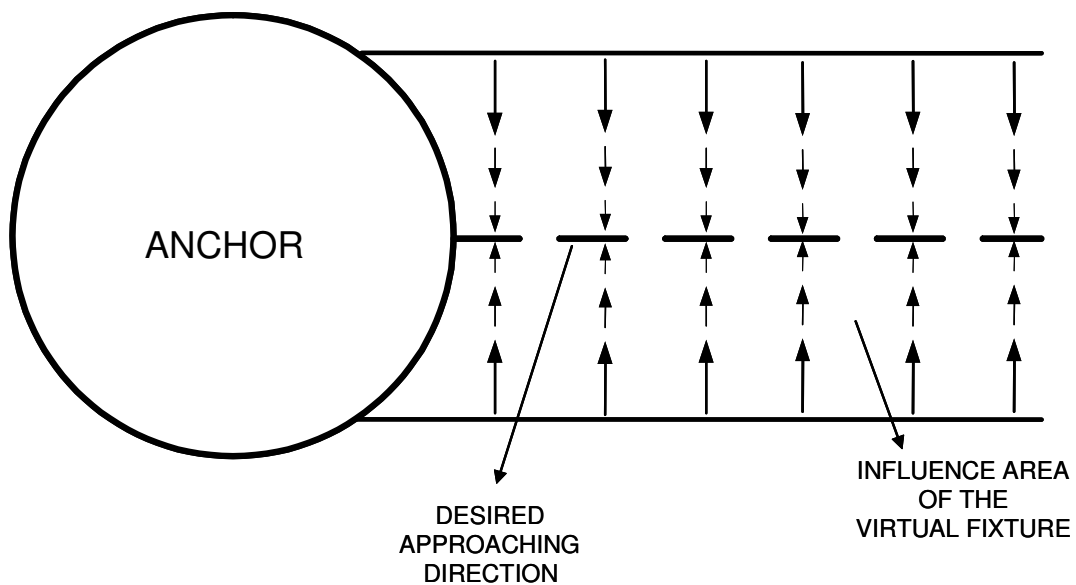


Figure 2.7 : During the binding of a biotin-coated particle to a streptavidin coated one (the anchor), a virtual fixture helps the user to maintain the necessary angle of approach. Linearly decreasing forces attracting the biotin particle towards the line of approach are displayed to the user through haptic device. Also, the repulsive field around the streptavidin particle prevents the user to apply excessive forces during the binding.

2.3.4 Constructing Microsphere Assemblies

In order to construct microsphere assemblies with different patterns, it is necessary to bind microspheres to each other. Currently, simple patterns can be formed by self-assembly. We suggest that more complex patterns can be constructed using OT and a haptic device using the proposed haptic manipulation and guidance techniques. In the past, binding of microparticles to each other have been accomplished using different mechanisms. The examples of these mechanisms include binding using DNA molecules [21], antibody-antigen bindings, protein-receptor bindings, and binding using hydrophobic interactions [22]. Since the particles in these examples are bound to each other via self-assembly, control on the pattern formation is very limited.

In our approach, binding of the microspheres to each other is accomplished via the protein-receptor mechanism. Particles coated with streptavidin molecule (protein) and biotin molecule (receptor) are chemically bound to each other. The streptavidin-biotin couple is commonly used for binding particles through self-assembly due to its extreme stability over a wide range of temperature and pH. The applications include flow cytometry, genetic mapping, and coupling of antibodies and antigens to agarose. In our application of constructing micro resonators, first, streptavidin coated microspheres are immobilized on the coverslip (i.e. anchor spheres). Then, a biotin coated microsphere is trapped by the OT and steered to bring close to a streptavidin coated microsphere with the help of path planning forces and haptic feedback. Finally, these two particles are bound to each other precisely with the help of virtual fixtures and haptic feedback again. The binding of the biotin to the suitable docking sides on the streptavidin occurs rapidly as a result of the strong affinity between those two (Figure 2.8a). Since the approaching angle of the microspheres to each other can be controlled by the user via virtual fixtures, patterns in desired geometries can be formed easily (Figure 2.8b)

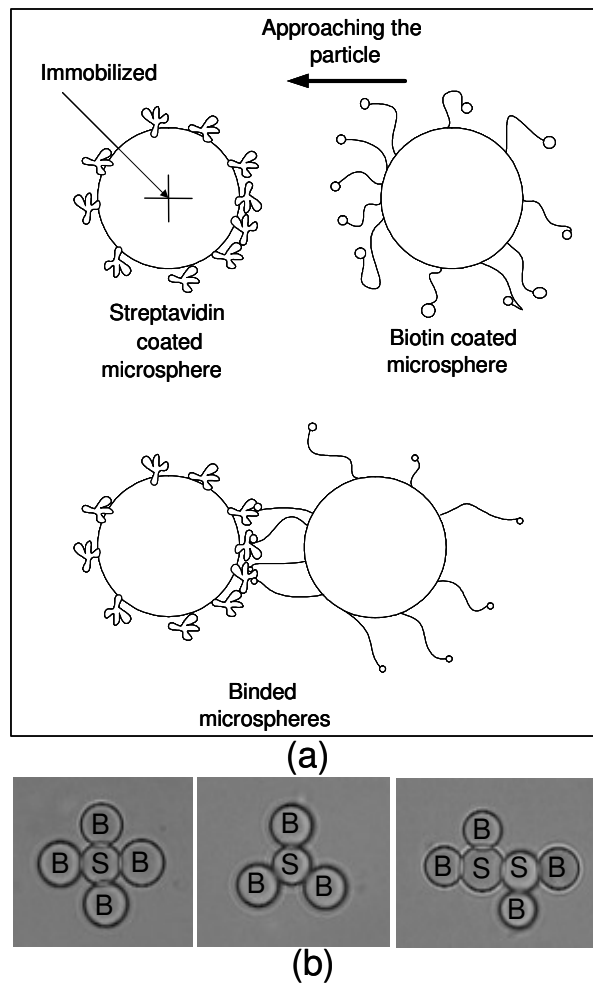


Figure 2.8 : a) Assembly of microspheres using biotin-streptavidin binding. If a biotin coated sphere is brought to contact with a streptavidin coated sphere, the binding of the biotin to the suitable docking sides on the streptavidin occurs rapidly as a result of the strong affinity between those two. b) Different patterns constructed using the set-up. “B” and “S” letters indicate biotin and streptavidin coated spheres.

Chapter 3

EXPERIMENTAL STUDY

In order to investigate the role of the haptic feedback in micromanipulation using OT, we have designed two different experiments with 8 human subjects. The goal of the first experiment was to analyze the performance of the subjects during the steering and binding of microspheres in virtual environments to construct a micro resonator with and without the help of haptic feedback. This experiment was conducted in a simulated world because it is impossible to generate the same manipulation environment and thus display equal conditions to all subjects in real world settings. In order to assemble microspheres using OT, a droplet of solution containing streptavidin and biotin coated particles is put on a cover slip first and then biotin coated spheres are trapped, steered, and bound to streptavidin coated particles. It is not possible to control the number of particles in the droplet and their distribution on the cover slip. Hence, it is impossible to display the same manipulation environment and the experimental conditions to all subjects especially during the steering of particles. For this reason, the simulation experiment is designed to test primarily the performance of users during the transfer of the trapped particle. On the other hand, the binding process is independent of the number and distribution of particles. A second experiment was conducted using the OT setup to investigate the subjects' performance during the binding process with and without the guidance of haptic feedback.

Eight subjects participated in the experiments conducted in virtual and real environments. In both experiments, there were two experimental conditions depending on

the type of sensory feedback provided to each subject. The sensory conditions are as follows:

- (1) Only Visual Feedback (V)
- (2) Visual + Haptic Feedback (V+H)

3.1 Experiment I

3.1.1 Goal

The goal of the first experiment is to assemble 4 dark blue spheres around an anchor sphere (light blue) in virtual environments as shown in Figure 9. The users are asked to pick each of the four dark blue spheres using their haptic device in the given order and steer it to the goal position displayed on the screen (pink sphere) for binding to the anchor sphere. They are asked to avoid making collisions with the green spheres (Figure 9) during the steering.

3.1.2 Design

There were a total of 20 trials for each experimental condition (V and V+H) and the experiments were performed in two sets with one week time interval between the sets. The subjects were divided into two groups (four in each). In the first set, the first group received ten trials with condition (2) (V+H) and then ten trials with condition (1) (V) while the second group received ten trials with condition (1) and ten trials with condition (2). After one week, the first group received ten trials with condition (1) and then ten trials with

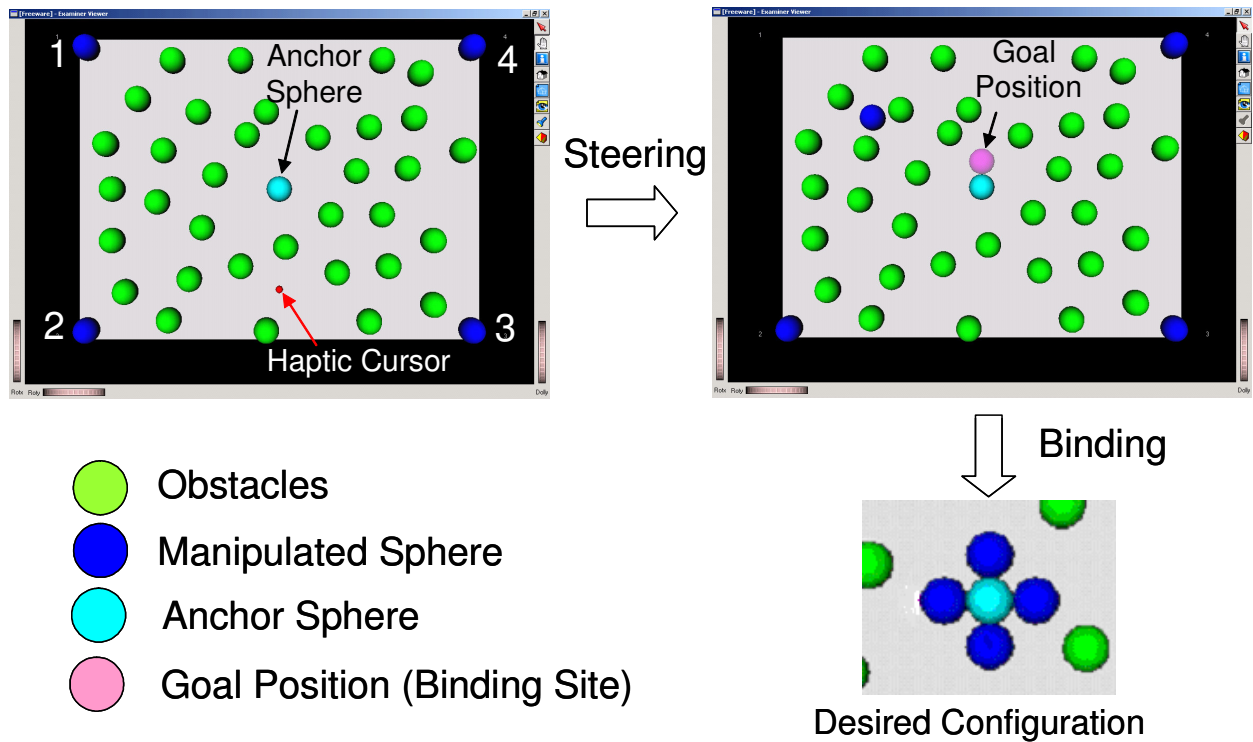


Figure 3.1 : The simulation window displayed to the subjects during Experiment I. The task is to steer each of the four blue spheres located at the corners of the cover slip (gray plane) and bind it to the anchor sphere (light blue sphere) located at the center to form the desired configuration.

condition (2) while the second group received ten trials with condition (2) and ten trials with condition (1) (Table 1). This matrix approach is used to eliminate the effect of the order of experimental conditions on the performance of the subjects

Table 3.1 : The matrix design for Experiment I. Subjects were divided into 2 groups (Group I and Group II), each having 4 members. The experiments were performed in two sets with one week rest interval between them. Each set consists of 20 trials. In set I, Group I performed the experiment 10 times under the condition 1 (V) first and then condition 2 (V+H) while Group II performed the experiment 10 times under the condition 2 (V+H) first and then condition 1 (V). In set II (one week later), groups repeated the same experiment in exactly the opposite order of sensory conditions.

	GROUP 1 (4)	GROUP 2 (4)
SET 1	V+H (10) → V(10)	V (10) → V+H(10)
	↓ 1 WEEK	↓ 1 WEEK
SET 2	V (10) → V+H(10)	V+H (10) → V(10)

3.1.3 Procedure

Before the experiments, subjects were given a handout explaining the goal of the experiment and containing step by step instructions about what they should do to accomplish the task. During the experiments, the subject moves the haptic cursor (shown as

a small red sphere in the screen) over the first dark blue sphere and presses the “S” key on the keyboard to pick it. Once the sphere is picked, the haptic device is virtually coupled to it and a transparent pink sphere appears on the screen, showing the goal position. Then the subjects steer the grabbed sphere by moving the haptic stylus to the goal position while avoiding collisions with other spheres (green spheres) in the scene. When the task is accomplished, the subject drops the sphere by pressing the “D” key on the keyboard. The same procedure is repeated for the other 3 dark blue spheres.

3.1.4 Results

A total of 6 different measures is defined to evaluate the performance of the subjects under two different experimental conditions. One of the measures is the task completion time which is the measure of the total time it takes to complete the task (i.e. the total time that passes between the picking and dropping of the four spheres). The rest of the measures can be classified into two groups. The first group of performance measures are related to the steering process and include contact duration and maximum penetration during steering. The contact duration during steering is the total time that the grabbed sphere is in contact with the obstacles (green spheres) during its transfer to the goal position. The maximum penetration during steering is the maximum distance the manipulated sphere penetrates into the obstacles during steering. The second group of performance measures are related to the binding process and include contact duration, maximum penetration, and maximum angular deviation during binding. The contact duration during binding is the total time that the grabbed sphere is in contact with the anchor sphere (light blue sphere). The maximum penetration during binding is the maximum distance the manipulated sphere penetrates into the anchor sphere during binding. The maximum angular deviation during binding is the maximum angle between

the line connecting the center of the anchor sphere and the goal position and the one connecting the centers of the anchor and the manipulated spheres while they are in contact. Those 6 measures are calculated for each trial and the mean values are used to compare the performance of the subjects under the experimental conditions of visual feedback only (V) and visual and haptic feedback together (V+H). The results are shown in Figure 3.2. The figure shows that Visual + Haptic (V+H) feedback together is significantly better than Visual (V) feedback only for all scores ($p < 0.001$). The haptic feedback improves both the speed and accuracy of the steering and binding processes. These results agree with the results of the earlier teleoperation experiments. We further investigated the effect of haptic feedback on task learning. For this purpose, the average task completion times of the subjects with and without haptic feedback are plotted against the number of trials. As shown in Figure 3.3, the task completion time under the condition (1), is not reduced as the number of trials are increased while there is an exponential decay under the condition (2) indicating that the task is being learning. An exponential curve in the form of $y = a e^{-bx} + c$ is fitted to the experimental data of the V+H condition ($R^2 = 0.996$). The curve reaches to the steady state, indicating learning has occurred, around 14th trial with 5 % relative error.

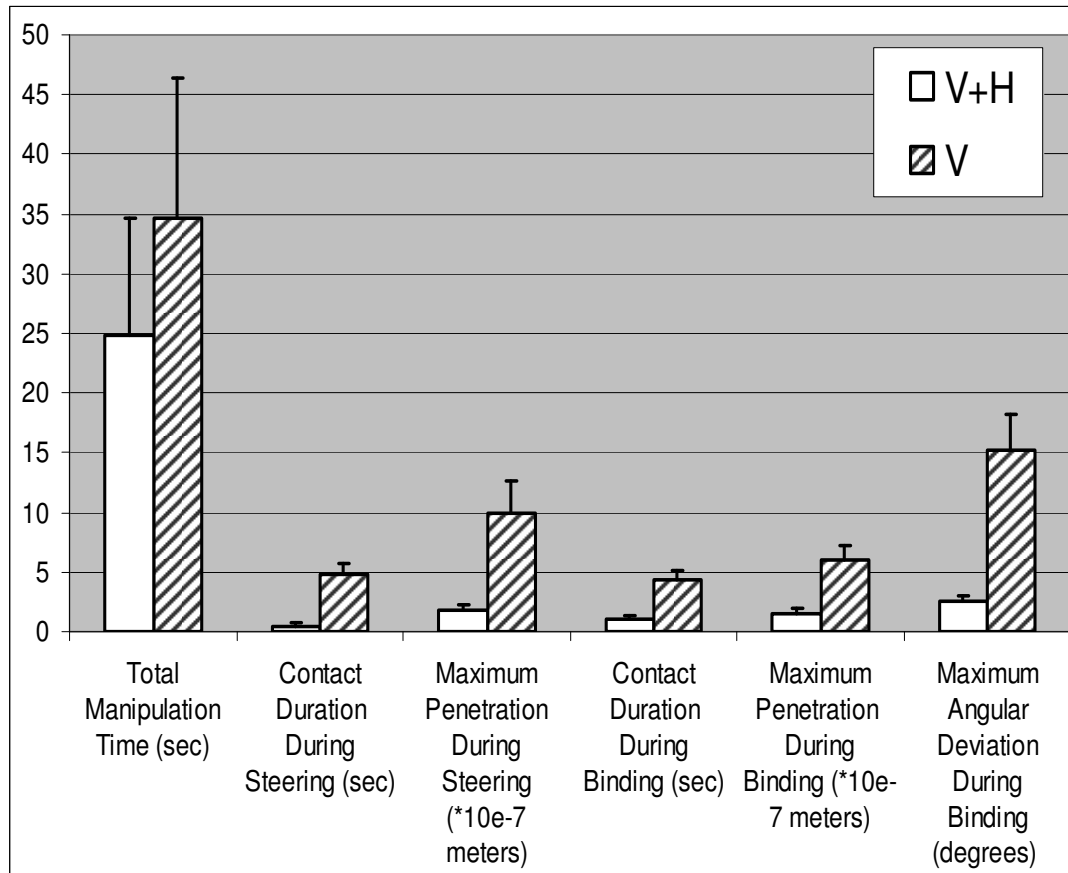


Figure 3.2 : The results of Experiment I conducted in virtual environments show that manipulating micro particles with haptic and visual feedback together (V+H) is significantly better than that of visual feedback only (V) in all aspects.

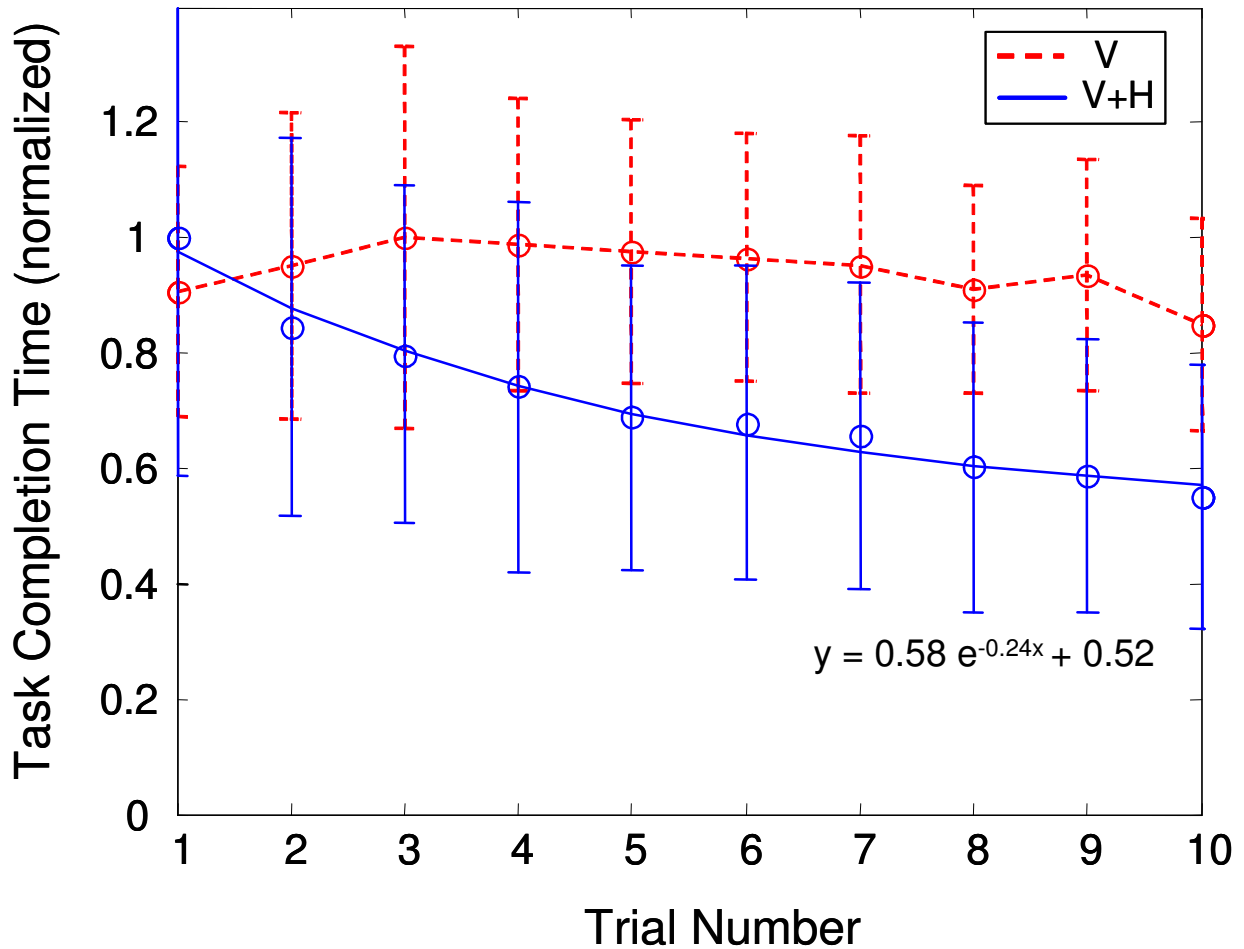


Figure 3.3 : The effect of haptic feedback on the task learning in Experiment I. The task completion times are plotted against the trial numbers. When visual feedback is displayed to the subjects only, learning does not occur (dashed lines). However, when the haptic feedback is added, the task completion time show an exponential decay indicating that the learning has occurred.

3.2. Experiment II

3.2.1 Goal

The goal of this experiment is to assemble 3 spheres by chemically binding two floating biotin coated particles to the left and right sides of a streptavidin coated particle fixed on the cover slip. Subjects are asked to form a horizontal line by carefully aligning the spheres. A perfect alignment is important for obtaining the desired emission spectrum of the resonator. The experiment was conducted in real environments using the OT set-up and the haptic device. In particular, we focused on the performance of subjects during the binding process since it is highly difficult to display the same manipulation environment to all subjects to investigate their steering performance.

3.2.2 Design

The same group of 8 subjects are participated in the experiments. The subjects are asked to construct exactly 10 microsphere assemblies under two sensory conditions (V and V+H) in random order. The order of the sensory feedback was random, but same for all subjects. The number of trials performed by each subject to construct the required number of resonators depended on his/her success in the task. For example, if the sphere escapes from the optical trap during steering or binding in an experimental trial, that trial is counted as “unsuccessful” and a new trial is started.

3.2.3 Procedure

To construct a microsphere assembly, the subjects trapped a bion particle, steered to the suitable binding site, and then bound it to the streptavidin coated microsphere by pushing. Subjects could easily differentiate a fluorescent streptavidin coated particle from a non-fluorescent bion coated one by simply directing the laser beam on it. The bion-coated spheres do not emit light and float in the solution. To trap a bion coated sphere, the subject manipulates the haptic stylus and brings the particle under the laser beam. Then, he turns the laser filter off (which is initially ON to prevent the particle escaping from the trap accidentally while approaching to the laser beam) to trap the particle by pressing the “W” key on the keyboard. If a bion particle is successfully trapped (if not, the subject presses the “E” key to turn on the filter again and searches for another particle), then the subject initializes the visual and haptic simulation by pressing the “S” key on the keyboard. In addition to the image window, a simulation window displaying the 3D simulated models of the particles shown in the image window is displayed. The subject steers the particle to the binding site while tracking its movements in the image and the simulation windows. The binding site is shown as a red sphere in the simulation window to guide the subject. The subject binds the bion coated sphere to the streptavidin coated one by pushing and mating them. Subjects are asked to test if the binding has occurred by lightly shaking the bion particle using the stylus of their haptic device. If he/she is convinced that the binding has occurred, he/she finalizes the task by pressing the switch on the haptic stylus. Figure 3.4 shows the manipulation screen during experiments

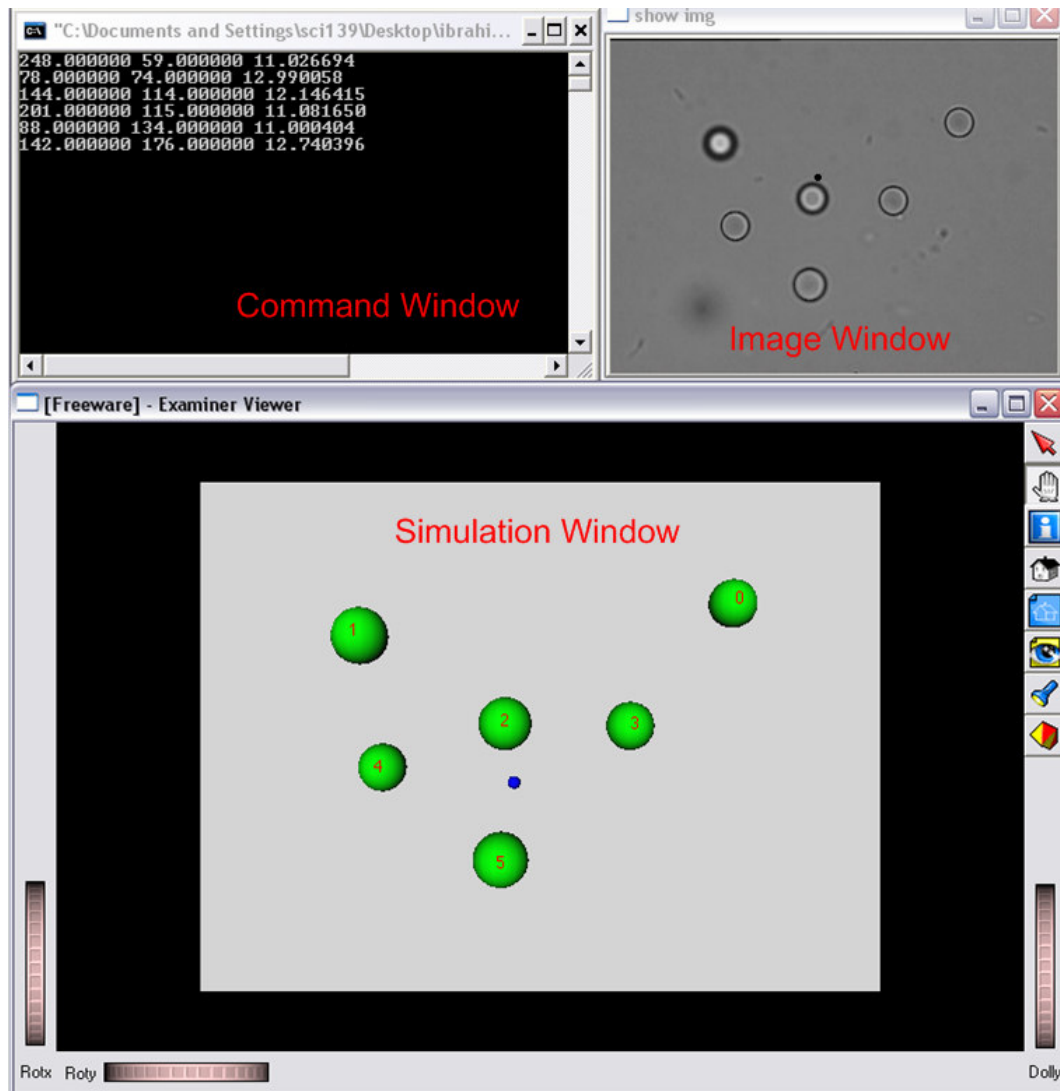


Figure 3.4 : Three windows displayed to the subjects during Experiment II: (1) The image window displays the real images of the particles being manipulated. (2) The simulation window augments the user's perception by displaying the bird's eye view of the manipulation environment and by highlighting the manipulated and anchor particles and the desired binding sites in different colors. (3) The command window enables the user to enter the inputs.

3.2.4 Sample Preparation

The biotin coated non- fluorescent microspheres with a diameter of 3-3.9 μm are purchased from Kisker-Biotec Inc. (ID : PC-B-03). The dragon green fluorescent microspheres with a nominal diameter of 3.69 μm (ID: FS05F) are purchased from Bangs Laboratories Inc and then coated with streptavidin (purchased from Prozyme Inc.) in the bio-technology laboratory of our school. We preferred to use fluorescent microspheres for two reasons: first, the spheres must be fluorescent in order to be used as optical resonator. Second, a fluorescent particle emits light when a laser with an appropriate wave length is directed on it and hence this feature can be used to differentiate streptavidin coated particles from the biotin coated non- fluorescent ones. The fluorescent microspheres are coated with streptavidin using a passive adsorption technique. First, 100 μl of solution containing microspheres is centrifuged at 6500 rpm for 5 minutes. At the end of the centrifugation process, the supernatant is removed and discarded. Then, the microspheres are resuspended in water and vortexed for mixing. Then this washing process is repeated for two times. But in the second run, the microspheres are resuspended in PBS with Ph = 7.4 instead of water. After the last washing, the appropriate amount of purified streptavidin (1 μl) is added to the microsphere solution and mixed gently for 2 hours at room temperature. Then the solution is left over night at 4 $^{\circ}\text{C}$. The process ends after the solution is washed again as before and resuspended in PBS again. The biotin coated microspheres are suspended in a different storage buffer than the streptavidin coated particles. In order to prevent the biotin coated particles sticking to the cover slip, we add 1% volume of BSA into the PBS solution.

To prepare the manipulation environment for our experiments we first placed the cover slip on the piezo scanner. Then, we dropped 25 μl of solution containing streptavidin

coated microspheres on the coverslip and waited until the microspheres stick to the coverslip surface. Finally, 25 μl of solution containing biotin coated microspheres is added.

3.2.5 Results

The total number of trials performed by each subject to construct the required number of microsphere assemblies under each sensory condition is considered as a measure of his/her success in performing the task (Table 3.2). As shown in the table, the number of trial performed by the subjects under the condition (1) is more than the one performed under the condition (2). The reason for the “unsuccessful” trials under the condition (1) is the escape of the particle from the trap during binding because of the excessive penetration to the anchor sphere. Two additional measures are defined to evaluate the performance of the subjects under each sensory condition: angular deviation during binding and the elevation difference between the bound sphere and the anchor sphere (Figure 3.5). The angular deviations of the biotin coated spheres bound to the streptavidin coated sphere from the left and right on the plane of cover slip (α_L and α_R) are measured from the image of assembly captured at the end of each successful trial. Then the average of the left and right angular deviations is reported. Similarly, the elevation difference between each bound sphere and the anchor sphere (Z_L and Z_R) are measured using the camera image and the movements of the scanner along the axis perpendicular to the plane of cover slip. The results (Figure 3.6) show that the average angular deviation and the elevation difference is significantly higher for the condition (1) when compared to the condition (2) ($p < 0.0001$).

Table 3.2 : The comparison of the success rates of the users in accomplishing the assembly of 3 spheres on a horizontal line under the conditions 1 and 2 in Experiment II The success rate increases with haptic feedback.

Subject	V Number of Trials	V+H Number of Trials
1	5/7	5/5
2	5/6	5/5
3	5/7	5/5
4	5/5	5/5
5	5/9	5/6
6	5/6	5/5
7	5/6	5/5
8	5/8	5/5
Total	40/54 (74%)	40/41 (97%)

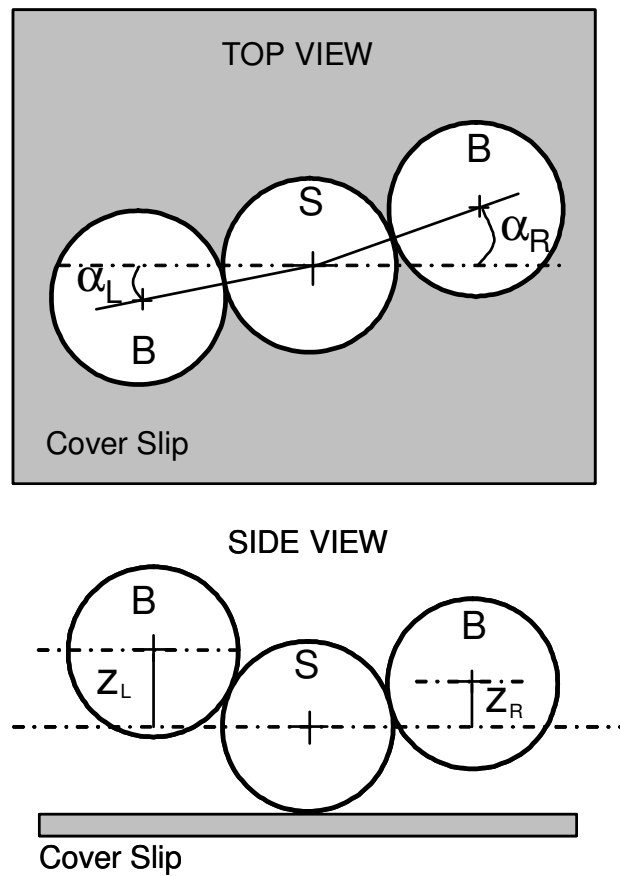


Figure 3.5 : The quantities measured in Experiment II. The image of the pattern constructed by the subject at the end of the binding task is processed to measure the deviations from the desired angle of binding (α_L and α_R) on the plane of the cover slip. Moreover, the deviations from the desired binding position along the axis perpendicular to the cover slip (i.e. parallel to the axis of the laser beam) are measured using the camera forces and the scanner movements along the same axis.

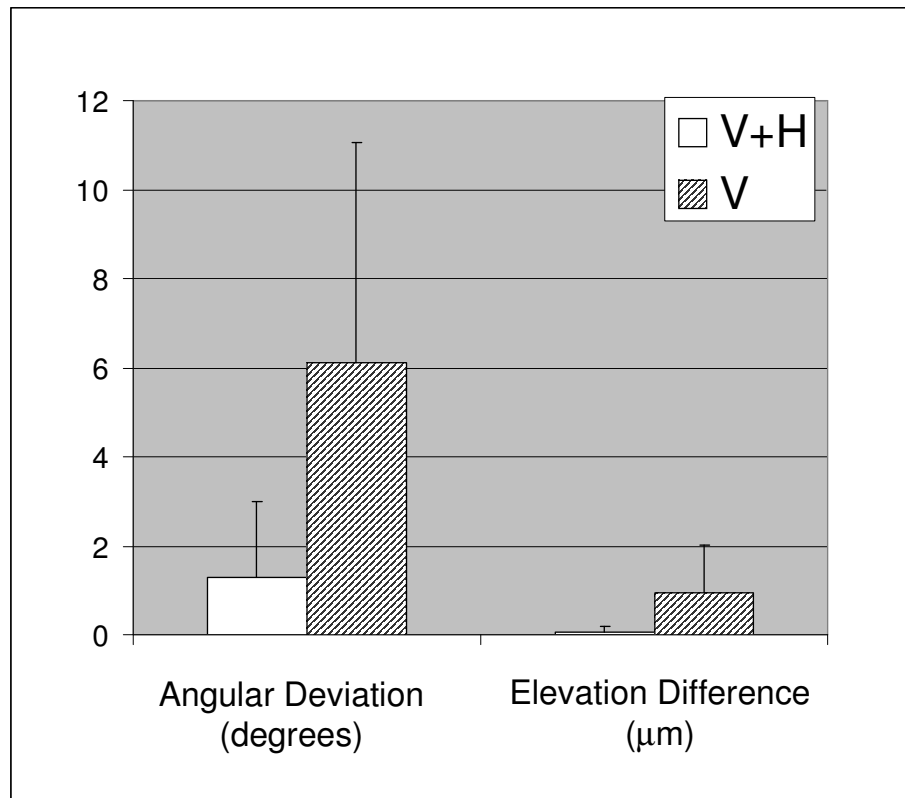


Figure 3.6 : The results of Experiment II conducted with the experimental OT set-up show that haptic and visual feedback together (V+H) is significantly better than visual feedback only (V) in assembling biotin and streptavidin particles to construct patterns.

Chapter 4

DISCUSSIONS and CONCLUSION

We developed a setup for manipulating and assembling microspheres which can be used to construct coupled resonators or coupled resonator optical waveguides (CROW) using OT and a haptic device. To our knowledge, this is the first time that a haptic device is coupled with OT to guide the user during an optical manipulation task involving steering and assembly of micro particles. Considering the fact that OT are used by several research groups to manipulate micro and nano scale objects in various applications, we hope that this thesis will stimulate the others to integrate haptic devices into their applications. In addition to our study, Lee et al propose a model to simulate force interactions between a particle and a laser beam for haptic manipulation of micro particles, but their work is purely theoretical and haptic forces are used to keep the particle in the trap only [23]. In our approach, in addition to displaying trapping forces to the user via a haptic device, an artificial potential field is used to help him/her steer the trapped particle to the desired location while avoiding collisions with the other particles in the scene. Then, a virtual fixture is used to bind particles to each other with high precision for constructing a coupled microsphere. The research in this area is recently focused on constructing geometries such as linear chains, 2D arrays, and 3D crystal structures. The techniques available today for this purpose include self assembly, self assembly on lithographically patterned surfaces, and individual manipulation of microspheres using tapered fiber probes, but none of them is sufficient for building complex structures with high precision. The patterns are formed

randomly with no control on the geometry in self-assembly. Moreover, electrostatic forces affect the positioning accuracy of the particles in invasive approaches using fiber probes. However, the performance of these structures as resonators depends on the size and positional accuracy of the assembled spheres which can have a profound, but not very well studied effect on optical transport [24]. Our personal communication with expert physicists in this area revealed that precise manipulation and alignment of spheres to form patterns for micro resonator construction is an open research problem. In this study, we show that OT augmented with haptic feedback could be an excellent candidate for the solution of this problem. We showed that displaying guidance and trapping forces to the subjects through a haptic device improved their performance in steering and binding processes significantly. To assemble the micro spheres, we used biotin-streptavidin binding which takes place rapidly. Hence, collisions during steering may lead to unintended binding if manipulations are performed with visual feedback only. The artificial repulsive force fields constructed around the obstacles (the particles along the manipulation path) and displayed to the subject through the haptic device prevents this from happening. These repulsive forces combined with the attractive forces pulling the trapped particle to the goal point generate a tunneling effect for easier manipulation. Our experiments conducted in virtual environments show that haptic guidance via an artificial force fields improves the user performance and learning significantly. Kuang, et al conducted path navigation tasks in virtual environments and also show that significant learning and training transfer occur with force field guidance of virtual fixtures measured by performance time and path length [25]. Another benefit of the haptic feedback is in the binding process. The repulsive field around the anchor particle prevents the user from applying excessive forces to it during binding. Moreover, a virtual fixture is used for the precise alignment of the binding particles. The virtual fixture exerts forces on the user to guide him/her towards a line such that the desired angle of approach is achieved. The results of our experimental study

conducted with OT and a haptic device show that binding without haptic feedback may cause elevation differences along the axis of laser beam between bound and anchor spheres as large as $3 \mu\text{m}$ (Mean = $0.93 \pm 1.07 \mu\text{m}$), which is significant compared to the diameter of the assembled spheres ($\sim 4 \mu\text{m}$). Moreover, the angular deviation on the plane of coverslip during binding can be as large as 20° degrees (Mean = $6.1 \pm 4.9^\circ$). These values are significantly lower when haptic feedback is present in the system ($0.05 \pm 0.15 \mu\text{m}$ and $1.3 \pm 1.7^\circ$). The results show that the desired patterns for micro resonators can be constructed more precisely using haptic feedback. In particular, the elevation difference, which also represent angular deviation in the plane perpendicular to the coverslip, is highly significant in condition 1 (V). We observed that subjects push the trapped sphere uncontrollably towards the anchor sphere for binding when there is only visual feedback. Due to the contact interactions, the trapped sphere may then go under or above the anchor sphere creating an elevation difference along the axis perpendicular to the coverslip. Since the camera displays the top views of the spheres, there is no visual feedback along this axis to adjust the position of the trapped sphere with respect to the anchor sphere. However, when there is haptic feedback, the artificial forces due to the repulsive field of the anchor sphere prevent the user to apply excessive forces during binding and the ones due to the virtual fixture keep the trapped sphere on the desired approaching direction. We should point that the effect of variations in the pattern geometry on the emission spectrum of the resonator is an open research problem (Astratov et al., 2004) and there are no published studies on that. In fact, even the concept of coupled microsphere resonators is new and only recently, Möller et al. demonstrated the existence of optical coupling for a micro resonator made of 3 spheres aligned on a line [16].

The steering and binding processes discussed in this thesis can be fully automated. However, more advanced image processing, computer recognition, and control techniques are necessary to identify the particle type (streptavidin versus biotin), to test if the particle

is mobile or not, to automate the trapping of a biotin particle, to track the positions of mobile particles in the scene all the time, and to test if binding has occurred or not. Alternatively, a shared control architecture such that automated steering and human-operated binding can be considered. However, the presence of a human operator in the steering task has an important benefit. It is known that the potential field approaches suffer from the local minima problem [27]. Hence, the manipulated particle may be trapped to the local minima and the task may be terminated without reaching the goal point. However, when a human operator is present in the loop, he/she can easily escape from the local minima by simply pushing the particle out of it and towards the right direction.

Following the binding and assembly, the fluid around the spheres must be dried to access the structure constructed. Because of the surface tension of the fluid, the constructed patterns may break or unwanted bindings of the surrounding particles to the constructed pattern may occur during drying.

BIBLIOGRAPHY

- [1] A. Ashkin, Acceleration and trapping of particles by radiation pressure, *Physics Review Letters*, 24 (1970), 156-159.
- [2] A. Ashkin, J. M. Dziedzic, J. E. Bjorkholm, and S. Chu, Observation of a single-beam gradient force optical trap for dielectric particles, *Optics Letters*, 11(1986), 288-290.
- [3] www.wikipedia.com.
- [4] K. Castelino, S. Satyanarayana, and M. Sitti, Manufacturing of two and three-dimensional micro/nanostructures by integrating optical tweezers with chemical assembly, *Robotica*, 23 (2005), 435-439.
- [5] A. Rohrbach, and E. H. K. Stelzer, Trapping forces, force constants, and potential depths for dielectricspheres in the presence of spherical aberrations, *Appl. Opt.*, 41 (2002), 2494–2507.
- [6] D. G. Grier, A revolution in optical manipulation, *Nature*, 424 (2003), 810–816.
- [7] Z. Bryant, M. D. Stone, J. Gore, S. B. Smith, N. R. Cozzarelli, and C. Bustamante, Structural transitions and elasticity from torque measurements on DNA, *Letters to Nature*, 424 (2003), 338-341.
- [8] P. J. Pauzauskie, A. Radenovic, E. Trepagnier, H. Shroff, P. Yang, J. Liphardt, Optical trapping and integration of semiconductor nanowire assemblies in water, *Nature*, 5 (2006), 97-101.
- [9] I. Bukusoglu, C. Basdogan, A. Kiraz, and A. Kurt, Haptic Manipulation of Microspheres Using Optical Tweezers, *Proceedings of 14th International Symposium on Haptic Interfaces for Virtual Environment and Teleoperator Systems*, 361-365 (2006), Arlington, Washington DC.
- [10] L. B. Rosenberg, Virtual Fixtures: Perceptual Tools for Telerobotic Manipulation, *Proc. of IEEE Annual Virtual Reality International Symposium*, (1993), 76–82.

-
- [11] S. Payandeh, Z. Stanisic, On application of virtual fixtures as an aid for telemanipulation and training, Proceedings of 10th IEEE International Symposium on Haptic Interfaces for Virtual Environment and Teleoperated Systems, (2002), 18 – 23.
- [12] A. Bettini, S. Lang, A. Okamura, and G. Hager, Vision Assisted Control for Manipulation Using Virtual Fixtures: Experiments at Macro and Micro Scales, Proceedings of the IEEE International Conference on Robotics and Automation, (2002), 3354-3361.
- [13] J. Aleotti, S. Caselli, and M. Reggiani, Evaluation of Virtual Fixtures for a Robot Programming by Demonstration Interface, IEEE Transactions on Systems, Man, and Cybernetics—Part A: Systems and Humans, 35 (2005), 536- 545.
- [14] K. Vahala, Optical microcavities. Nature, 424 (2003) , 839-846.
- [15] J. D. Eversole, H. B. Lin, and a. J. Campillo, Input/output resonance correlation in laser-induced emission from microdroplets, Journal of Opt. Soc. Am. B, 12 (1995), 287-296.
- [16] B. Möller, U. Woggon, and M.V. Artemyev, Photons in coupled microsphere resonators, Journal of Applied Physics, 8 (2006), 113-121.
- [17] K. Visscher, S. P. Gross, and S. M. Block, Construction of multiple-beam optical traps with nanometer-resolution position sensing, IEEE Journal of Selected Topics in Quantum Electronics, 2 (1996), 1066-1076.
- [18] K. Svoboda and S. M. Block, Biological applications of optical forces, Annu. Rev. Biophys. Biomol. Struct. , 23 (1994), 247-285.
- [19] O. Khatib, Real-time obstacle avoidance for manipulators and mobile robots, The International Journal of Robotic Research, 5 (1986), 90-98.
- [20] J. J. Abbott and A. M. Okamura, A. Virtual fixture architectures for telemanipulation, Proceedings of the 2003 IEEE International Conference on Robotics & Automation, (2003), 14-19.

-
- [21] C. A. Mirkin, R. L. Letsinger, R. C. Mucic, and J. J. Storhoff, A DNA-based method for rationally assembling nanoparticles into macroscopic materials, *Nature*, 382 (1996), 607-609.
- [22] H. Onoe, K. Matsumoto, I. Shimoyama, Three dimensional micro self assembly using hydrophobic interaction controlled by self assembled monolayer, *Journal of Microelectromechanical Systems*, 13 (2003), 603-611.
- [23] Y. Lee, K. W. Lyons, and T. W. LeBrun, Virtual environment for manipulating macroscopic particles with optical tweezers, *Journal of Research of the National Institute of Standards and Technology*, 108 (2003), 275-287.
- [24] V. N. Astratov, J. P. Franchak, S. P. Ashili, Optical coupling and transport phenomena in chains of spherical dielectric microspheres with size disorder, *Applied Physics Letters*, 85 (2004), 5508-5510.
- [26] A. B. Kuang, S. Payandeh, Z. Bin, F. Henigman, and C. L. MacKenzie, Assembling virtual fixtures for guidance in training environments, *Proceedings of 12th IEEE International Symposium on Haptic Interfaces for Virtual Environment and Teleoperated Systems*, (2004), 367 – 374.
- [27] Y. Koren, and J. Borenstein, Potential field methods and their inherent limitations for mobile robot navigation. *Proc. International Conference on Robotics and Automation*, Sacramento, CA, 1991, 1398-1404.

VITA

Ibrahim Bukusoglu was born in İzmir, Turkey on September 13, 1981. He received his B.S. degree in Mechanical Engineering for Middle East Technical University (METU), Ankara, in 2004., He has then enrolled to the M.S. program in Mechanical Engineering at Koç University as a teaching and research assistant. He has been working on the haptic manipulation with Optical Tweezers since September 2004. He is planning to continue his career as a Mechanical Engineer in the industry.